Forensic Imaging, Volume 30, September 2022, Article number 200510
DOI: 10.1016/j.fri.2022.200510

Title:

Cone cracking in human bone: A CT case review series

Authors:

Angi M. Christensen, PhD, D-ABFA[a] (corresponding author)

John M. Rickman, PhD[b]

[a] Federal Bureau of Investigation Laboratory; Quantico, VA; USA

amchristensen@fbi.gov

[b] Cranfield Forensic Institute, Cranfield University; Shrivenham; UK

Disclaimer:

This is publication number 21-33 of the Laboratory Division of the Federal Bureau of Investigation (FBI). Names of commercial manufacturers are provided for information only and inclusion does not imply endorsement by the FBI or the U.S. Government. The views expressed are those of the authors and do not necessarily reflect the official policy or position of the FBI or the U.S. Government.

Ethical approval:

This case review was fully authorised by the ethics committee of Cranfield University.

Abstract

Skeletal trauma analysis often involves the assessment of the types and patterns of fractures, followed by categorizing the trauma into one of several broad "mechanisms." Trauma analysis ideally also involves understanding the underlying mechanistic basis for the bone's failure. Beveling in bone is one example of a fracture pattern that is often cited as evidence of a high-velocity projectile impact, but appears to be poorly understood in terms of both the mechanism for bevel production as well as the loading conditions responsible for its formation. It has recently been demonstrated that bone beveling results from a failure mechanism called cone cracking, which is also associated with lower velocity impacts. Many case reviews and instructional texts include imagery of beveled bone in association with projectile impacts, but present various other explanations (or no explanation) for the fracture mechanism responsible. Five cases are presented here involving cone cracking in human forensic cases. For each case, the associated fracture patterns are discussed, photographic and micro-CT imagery are shown, and a review of the cone crack is presented in cross-section. The diagnostic utility of CT examination of ambiguous perforations is also highlighted.

Keywords

Skeletal trauma; forensic anthropology; forensic radiology; computed tomography (CT), fractography, cone cracking

Introduction

Skeletal trauma analysis in forensic contexts frequently involves looking for patterns that are typically associated with a particular "mechanism" or implement that impacted the bone, but there is often little or no consideration given to the fracture mechanics involved in bone failure. This typical (and largely typological) approach often does not take into account what is known about brittle material failure, or the continuum of failure patterns that may be observed as a result of skeletal trauma events.

Beveling in bone is one example of a fracture pattern that is often cited as evidence of a high-velocity projectile impact, being a circular fracture with an associated conoidal bevel flaring in the direction of projectile travel [1]. This pattern, however, has to date been poorly understood both in terms of the mechanism underlying bevel production and the loading conditions responsible for its formation. Failure mechanisms and resulting fracture patterns are well understood for many brittle materials impacted or perforated by projectiles such as glass and ceramics (see, for example, [2]. When impacted by a projectile, these materials are known to fracture in a pattern referred to as a *cone crack*. A cone crack is a conoid-shaped fracture resulting from an object impacting (including passing through) a brittle material. Despite the morphological similarities between these cracks and beveling in bone, cone cracking has been given little consideration by anthropologists, and many explanations for bone bevel formation are inconsistent with brittle material fracture mechanics and experimental observations. It has recently been suggested, and demonstrated by experimental evidence, that cone cracking is the fracture mechanism responsible for bevel formation in bone [3-4, summarized in 5].

Cone cracking was first described by Hertz [6] in the late nineteenth century and is therefore sometimes referred to as Hertzian cone cracking. An applied load from an impactor will reach a critical value and a circular-shaped crack, referred to as a ring crack, will form in the zone of maximum tension located just outside of and concentric with the indenter contact radius [7-8]. This ring crack will propagate for a short distance along a path normal (perpendicular) to the greatest tensile stresses, and will then propagate outward, flaring into a cone (Fig. 1). A cone crack will form from impact regardless of whether the projectile actually perforates the impacted material. When a cone crack propagates the full thickness of a structure, a cone-shaped piece of material (called a conoid) is formed, and a cone-shaped void that displays a part-counterpart relationship with the conoid is left behind. At lower velocities, the conoid may remain intact; if the projectile perforates the material, the conoid is typically comminuted [9]. In an experimental series impacting sandwich bones, no intact conoids were observed above 90 m/s [4]. However, partial remnants of the conoid may remain even after comminution in the form of inner cortical plate fragments displaying part-counterpart relationships with the bevel [3].

Figure 1: Schematic of cone crack formation (from [5])

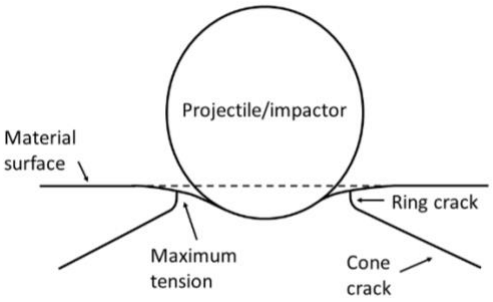

In support of this, beveled fractures have been observed in bone subsequent to blunt and low velocity projectile impact in human cranial material (e.g., see [10-12]), and have been generated

experimentally in non-human long bones [13] and sandwich bones [4]. Intact bone conoids have been described in both case [14-16] and experimental series [4].

Additional complexity is added to cone crack propagation through sandwich bones due to the presence of a cellular solid of variable thickness (the trabecular lamina) between the inner and outer cortical plates. Previous experimental work examining the fractured edges of the trabecular cells with micro-computerized tomography (μ-CT) has indicated that, once the cone crack has entered the cellular solid via trabecular struts that are in line with the region of greatest tensile stress, it crosses the cells by hopping from one cell edge to another under a combination of both tensile and shear stresses [3-5]. This trans-laminar fracture mechanism results in a continuous, typically straight-edged fracture margin from the cortical entry to the cortical exit [3].

Morphological features visible with CT and nomenclature for analysis

A cone crack that produces a bevel results in several morphological features that are discernible in cross-section with different forms of computerized tomography. A nomenclature for these features, developed for beveled entry fractures in porcine scapulae utilizing μ-CT [3], is adopted in the present paper (Fig. 2). In this nomenclature, a beveled entry fracture in sandwich bones has a *cortical entry* in the outer cortical plate and a *cortical exit* in the inner cortical plate (these are reversed in beveled exits). The medial margin of the cortical entry is defined as the *entry cortical fracture edge* (EnCF) and the same edge in the cortical exit is the *exit cortical fracture edge* (ExCF). These fracture edges typically exhibit angulation with respect to their associated cortical surface (CS), and in straight-edged fractures through the three laminae, the ExCF is in-line with the EnCF. Although such angulation is the norm, in some cross-sections through a given

perforation angulation may be reduced or absent, possibly reflecting the effects of compact bone microarchitecture in relation to the stress field. The free, fractured edges of the trabecular cells form the *trabecular fracture margin*, while the cells up to 3 mm peripheral to this edge form the *peripheral trabeculae*. Although typically straight edged, portions of the trabecular fracture margin may intrude into the conoidal void due to deviation in crack path as it crosses the trabecular cells (trabecular intrusion). The EnCF, trabecular fracture margin, and ExCF together define the internal conoidal *volume* of the perforation, and the trabecular fracture margin and ExCF define the *internal bevel* (external bevel in exit fractures).

Figure 2: micro-CT image showing cross-sectional anatomy of a projectile impact that perforated a sandwich structure bone (from [3])

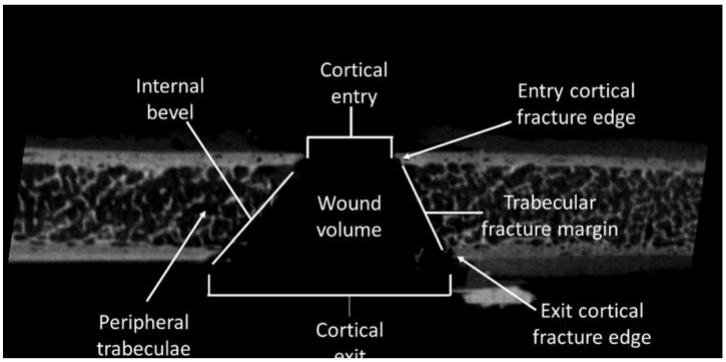

Recent years have seen the growing recognition that skeletal trauma exists on a biomechanical continuum, with fracture morphology dependent upon such factors as loading rate and the surface area of the impacting object [17]. Projectile trauma is a particularly good example of this phenomenon, with beveled defects forming during both low and high-velocity impact events. The biomechanical continuum poses important diagnostic challenges, particularly in the absence of a recovered projectile or when skeletal remains are taphonomically altered. Although internal and external beveling are readily visualized with CT, to date no forensic case-based study has utilized

this technology to examine their detailed cross-sectional structure. Accordingly, the cases discussed in the present paper will identify the morphological features associated with cone crack propagation and highlight the utility of CT analysis in the process of differential diagnosis. We suggest that a more thorough, mechanics-based understanding of bevel formation will enhance skeletal trauma analyses, providing greater insight into this fracture mechanism.

Case Reviews

Five cases are presented involving cone cracking in human forensic cases. For each case, the associated fracture patterns are discussed, photographic and micro-CT imagery are shown, and a review of the cone crack is presented using the cross-sectional morphology discussed above. All imaging was performed using a North Star Imaging X5000 digital radiology system and reconstructed using associated proprietary software. Settings varied somewhat for each case, but generally were around 175-200 kV, 150-300 mA, 500 projections, 4 frames averaged, with a 100 ms delay. The instrument and parameters used in this case review were selected because they are part of the imaging protocol used at the [institution redacted], and have been demonstrated to be useful in forensic anthropological analyses [18]. It is recognized that this imaging modality differs from those used in most postmortem imaging contexts, but it is expected that similar analyses can be performed, especially if resolution is maximized in the region of interest.

Case 1: Projectile impact of the occipital squama

Human skeletal remains were discovered along the side of a hill by someone walking their dog, and subsequently collected by representatives from the local sheriff and coroner offices. Bullet casings were also recovered from the scene. Following an initial assessment of the remains by a forensic pathologist, the case was referred for an anthropological analysis.

The cranium was received as four portions; one consisting of most of the cranial vault and facial skeleton (as pictured in Fig. 3), one consisting of a large section of the right cranial vault (including the right temporal and zygomatic, and portions of the right parietal, sphenoid, occipital, and frontal bones), as well as a right occipital squama fragment, and a fragment of the occipital bone lateral to the right occipital condyle. These were temporarily reconstructed using adhesive for imaging and analysis.

Figure 3: Largest of the cranial portions from Case 1, as received, in anterior (left) and posterior (right) views

Upon reconstruction and examination of gross morphology and CT imaging, a minimum of two projectile impacts were identified (a third impact was also noted on the mandible, though may be associated with the trajectory of one of the other impacts). Based on intersecting cracks, the first impact (not pictured here) involved the inferior/petrous portion of the right temporal as well as

portions of the inferior right occipital squama. The second impact, which produced the cone crack further analyzed here, involved the central occipital squama. The impact resulted in an elongated and internally beveled region of missing bone just left of the mid-sagittal plane, with the shape suggesting an angled impact. or projectile yaw or deformation. Three radial cracks emanate from the cortical entry (Fig. 4); one arises from the left edge of the cortical entry and terminates in the left lambdoidal suture approximately midway between lambda and asterion; a second arises from the top edge of the cortical entry and terminates in the lambdoidal suture superior to the first radial crack; a third radial crack arises from the top right edge of the cortical entry and branches near the origin, with the superior branch extending through the right occipital squama and right parietal eventually terminating near the right orbit, and the inferior branch terminating into a crack of the occipital squama associated with the first projectile impact. Radiodense material is also noted in the CT imaging on the right superior and inferior entry margins.

Figure 4: CT images of the reconstructed cranium from Case 1, showing projectile alterations including perforating cone crack, radial cracks, and radiodense material

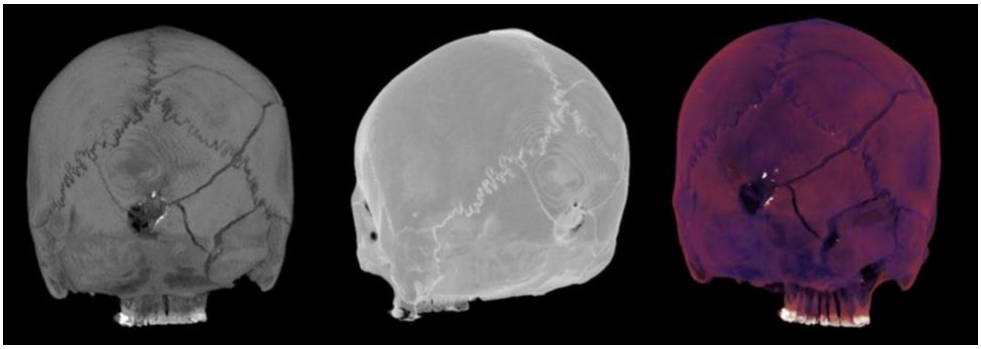

The cross-section of the cone crack in CT (Fig. 5) shows that the superior edge has propagated through a relatively thin portion of the occipital and the inferior edge has propagated through a thicker region involving the internal occipital protuberance. Despite the greater thickness in this part of the cone crack, the trans-laminar fracture has resulted in a straight-edged fracture margin

extending from the cortical entry to the cortical exit. Both the superior and inferior EnCF are angulated at approximately 45° with respect to the cortical surface. Despite the greater thickness of the inferior cone crack edge, the trans-laminar fracture through the three layers has resulted in a fairly symmetric internal conoidal morphology. Damage is characteristically localized to the perforated region (i.e., there is no trabecular compression, densification, delamination, or crushing of the cortex).

Figure 5: CT-derived cross-sectional views of the cone crack in Case 1 showing angulation of crack margin through the three layers of bone

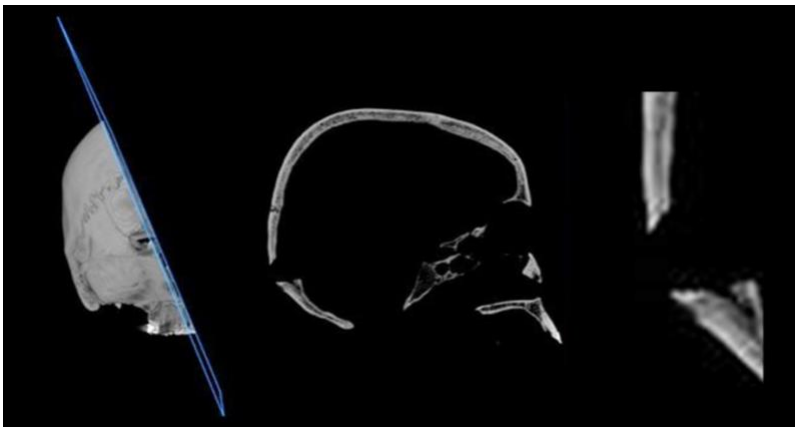

Case 2: Large cone crack from blunt impact to right parietal

Remains were discovered partially decomposed and with associated clothing. Apparent sharp alterations were noted on the clothing and soft tissue in the chest and abdominal regions, and a large defect was noted in the cranium, prompting evaluation by a forensic anthropologist. According to various accounts (including statements made by one of the suspects while in jail on another charge), multiple individuals stabbed the victim with a knife. When the victim survived the stabbing, one of the suspects struck the victim twice in the head with a hammer. A framing

hammer recovered from a suspect's vehicle was examined and compared to the cranium by a toolmark examiner following the anthropological analysis, and it was concluded that the cranial defects could have been caused by this hammer or a similar tool.

The cranium was received as multiple portions including most the cranium and several vault fragments which were temporarily reconstructed using adhesive (Fig. 6). Two primary areas of alteration are revealed, one consisting of a roughly circular alteration in the right cranial vault (further reviewed here) and one consisting of missing and fractured bone in the right facial region. The circular alteration is an internally beveled cone crack (Fig. 7) involving the right parietal and part of the right temporal squama. There are three primary radial cracks; one extending antero-inferiorly through the right temporal squama (bisecting the temporal squama and resulting in a dislodged fragment), one extending antero-superiorly through the right parietal toward the coronal suture, and one extending postero-superiorly through the right parietal, crossing the sagittal suture and terminating in the left parietal. There is no corresponding exit opposite the beveled perforation, and the overall pattern is consistent with blunt trauma. In this case CT imaging was especially beneficial in identifying the presence of beveling, which may not have been suspected based on the ectocranial trauma pattern, and is best visualized in endocranial and cross sectional views.

Figure 6: Largest of the cranial portions from Case 2, as received, in anterior (left) and right lateral (right) views

Figure 7: CT imaging of the cone crack in Case 2, including cutaway/slice view showing internal beveling (right)

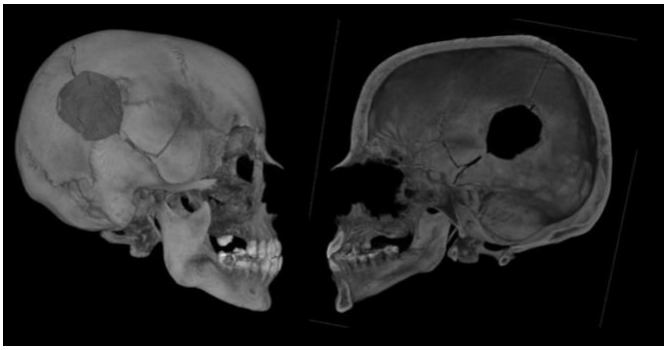

In the superior aspect of the defect, the crack has perforated the three laminae of the parietal, with the crack increasing in angle approximately midway through the trabecular lamina (Fig. 8). The trabeculae in this region show no sign of compression, and the crack can be seen to have hopped from one cell to another as it propagated through the trabecular laminae under tension. At the inferior aspect of the defect, the cortical bone is thin and lacks a substantial trabecular lamina. Despite the thin bone in this region, there is still clear angulation of the crack with respect to the cortical surface.

Figure 8: CT-derived cross-section of the cone crack in Case 2 showing angulation of the margins

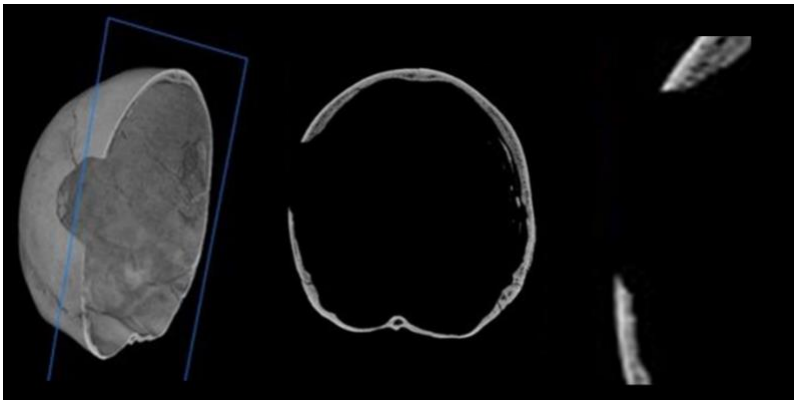

Case 3: Cone crack along lambdoidal suture

Department of Transportation employees performing road work discovered skeletonized human remains including two crania with apparent projectile trauma. The area where the remains were discovered was near the recovery location of a vehicle involved in a carjacking related to five suspected homicides the previous year. During the initial recovery of several other victims and the vehicle, .22 caliber casings were found near the recovery scene and in the vehicle. The crania were referred for anthropological examination.

One of the crania (reviewed here) was received largely intact, and displays an irregular perforating defect along the right lambdoidal suture, just adjacent to lambda (Fig. 9). This location (combined with the irregular shape of the perforation) necessitates differential diagnosis from a missing sutural ossicle. When viewed externally, this taphonomic alteration can mimic projectile trauma very effectively, particularly when associated with additional fractures potentially representing the region of exit [19].

Figure 9: Cranium from Case 3, as received, in posterior view (left) showing the perforation, and right lateral view (right) view showing the alterations to the right temporal region

There are no radial or circumferential cracks associated with the perforation in this case, and radiodense debris can be seen on the margins in the CT imaging (Fig. 10). There is also a region

of missing, fractured, and hinged bone affecting the right temporal squama, sphenoid, frontal, and zygomatic. Two primary radial cracks emanating posteriorly from this region, one extending into the right parietal, terminating prior to the sagittal suture, and a second extending through the squamous portion of the right temporal and terminating superior to the mastoid process. A third radial crack extends across the right side of the frontal bone, branching above the right orbit. CT imaging also reveals the presence of an apparent projectile remnant adjacent to the perforation. At the time of the anthropological examination, this material was removed and referred for metallurgy analysis and determined to have a similar alloy composition to recovered cartridges.

Figure 10: CT imaging of Case 3 showing radiodense debris around the perforation (left), frontal bone fractures (middle), and projectile remnant (right)

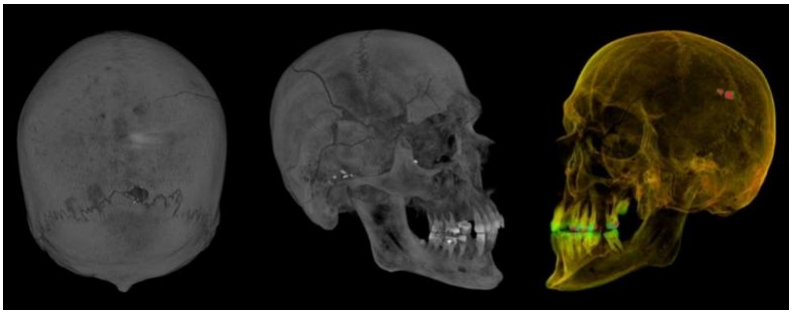

The perforation in this case is a cone crack exhibiting internal bevelling in both sagittal and transverse sections (Figs. 11-12). The cross-sectional morphology of the inferior part of the entry differs from the superior part due to it being formed by the lambdoid suture. The bevelled regions exhibit features associated with cone crack propagation including angulation of the EnCF, in-line fracture from the EnCF to the ExCF, straight-edged fracture margins, and lack of delamination of the sandwich bone laminae. Together, these features are consistent with the perforation being an internally bevelled projectile entry, with the alterations to the right temporal and orbital region consistent with a projectile exit.

Figure 11: CT-derived sagittal cross-section of the cone crack in Case 3 showing projectile remnant (left, middle) and edge of lambdoidal suture (right, lower aspect of perforation)

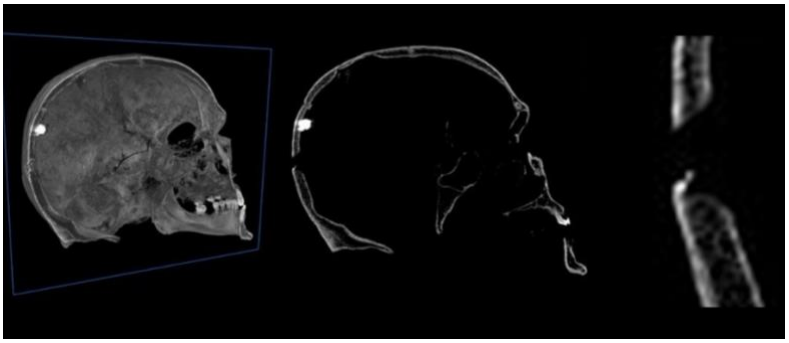

Figure 12: CT-derived transverse cross-section of the cone crack in Case 3 showing angled fracture margins and lack of cortical lining of the perforation (since this section is superior to the lambdoidal suture)

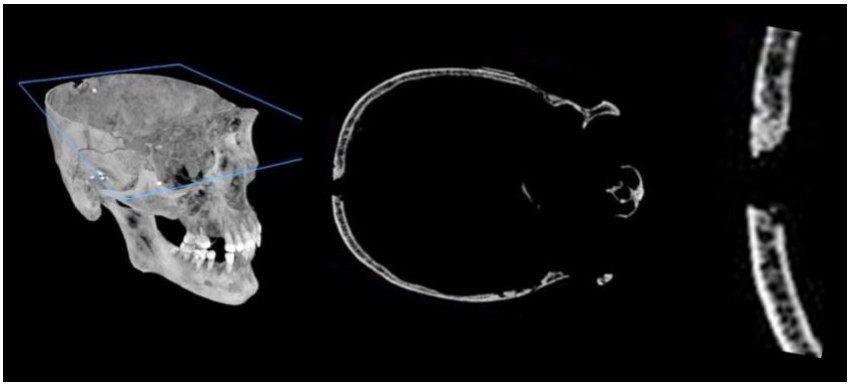

In transverse section (Fig. 11) there is no evidence of a cortical lining of the defect which would be expected with missing sutural ossicles [20], and the trabecular fracture margin induced by trans-laminar fracture is clearly visible. In terms of differential diagnosis, analysis of the cone crack through the use of CT imaging excludes a missing sutural ossicle and confirms that the perforation resulted from projectile perforation.

Case 4: Cone crack revealed following fragment reconstruction

Decomposing remains were discovered in a residence. Upon discovery, the head was thought to be absent, but recovered bone fragments were later determined to be cranial bones. A dog and cat were also in the residence, and it was presumed that they consumed some of the tissues of the head and neck. The initial autopsy identified perforating gunshot wounds of the torso and left arm. The cranial fragments were submitted for anthropological assessment to determine whether they might also exhibit evidence of projectile trauma.

The cranium is extensively comminuted and was received as 13 bone fragments (Fig. 13, upper left) which were temporarily reconstructed using adhesive. The fragments reconstruct well with show little to no signs of plastic deformation, consistent with their formation at high loading rates [21]. Upon reconstruction, large parts of the lower and anterior cranium are missing (some of the fracture margins were noted to have pitting and scoring consistent with scavenging), and a circular perforation in the occipital is revealed. The perforation in the occipital is bevelled internally and is thus identifiable as a projectile entry. Three radial cracks emanate from the entry (Fig 14); one extends superiorly, crossing the lambdoidal suture, another extends to the left with the termination complicated by missing bone, and a third extends inferiorly and to the right, branching after a short distance. The right parietal exhibits two large concentric cracks that arrest in the preceding radial cracks

Figure 13: Case 4 cranial fragments as received (upper left), and as reconstructed in anterior (left) and superior (right) views

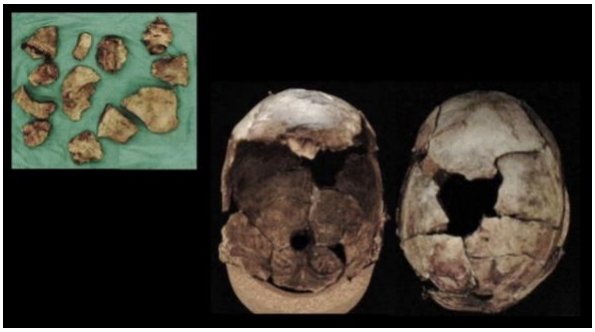

Figure 14: CT images of Case 4, showing cone crack, radiating cracks, and concentric cracks

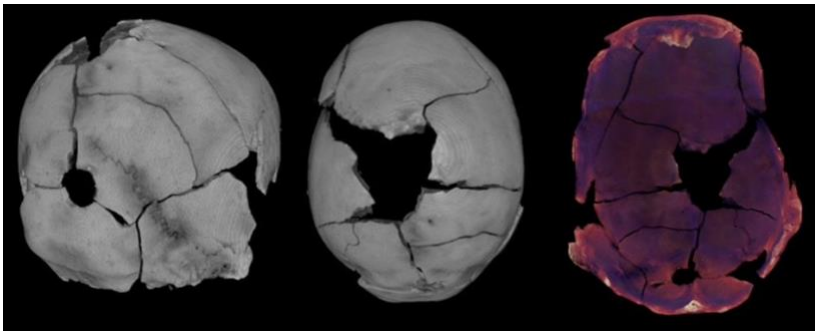

In sagittal section, one of the concentric cracks is seen to be externally bevelled in relation to the entry (Fig. 15, middle), consistent with being a concentric heaving fracture resulting from temporary cavitation due to projectile passage and resultant tensile failure of the inner cortical plate [22-23]. The inferior aspect of the cone crack has perforated through a region with no trabecular lamina, and the edge of the crack is straight. The superior part of the cone crack has crossed through a region composed of all three laminae and exhibits a small amount of trabecular intrusion into the volume due to deviation in crack path across the trabecular cells. There is no macroscopic delamination and the damage at the perforation site is limited to the displaced conoid; where the peripheral trabeculae are visible, they do not appear compressed or fractured. Overall, extensive comminution, cone crack formation, and concentric heaving fracture are consistent with projectile trauma involving extensive temporary cavity formation.

Figure 15: Figure X: CT-derived cross-section of the cone crack in Case 4, showing angled fracture margins of the cone crack, as well as a beveled concentric fracture (middle, indicated with an arrow) consistent with a heaving fracture

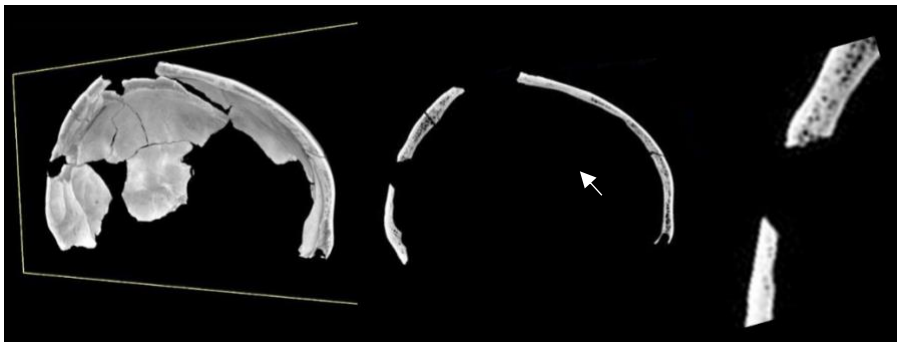

Beveling associated with circumferential/concentric crack has been documented previously. The angle/direction of the bevel can be used to differentiate between forces originating from the ectocranial surface (such as the inward bending of radially segmented fragments) versus the endocranial surface (such as in the outward bending of bone due to the cavity created by a passing projectile, as seen in this case) (see for example, [23]). The angle is influenced by shear forces and which end of the bone is 'fixed' [24,5].

Case 5: Cone crack in a mandible

Remains were recovered from a grave approximately 3 m deep. Prior to burial, the suspect reportedly shot the decedent, attempted to destroy the remains by burning them for three days using an accelerant, and then buried the body using a trackhoe. Thermal alterations were present on the skull and torso, and the case was referred for forensic anthropological analysis for a trauma assessment.

Thermal alteration of skeletal material was noted to primarily affect the left side of the body while some bones exhibited no thermal alteration. The cranium and mandible were highly fractured, and due to thermal alterations and the extent of missing bone, the trauma assessment of the cranium was inconclusive. The mandible (further assessed here) was reconstructed from five fragments, with discoloration representing thermal alteration focused on the anterior and left lateral mandibular body (Fig. 16). The mandible exhibits two perforating defects, one on the right inferior mandibular body and involving part of the right gonial angle, and one on the left inferior mandibular body just anterior to the gonial angle (Figs. 16-17). The right perforation is irregular in shape and exhibits one radial crack extending antero-superiorly across the oblique line. The left perforation is roughly circular superiorly, flaring outward inferiorly, and exhibits two radial cracks, one extending superiorly to the region of the extra-molar sulcus and one extending antero-inferiorly along the corpus. This left perforation is a cone crack exhibiting external bevelling, indicative of a medial to lateral impact direction, an interpretation consistent with a projectile entry on the right side and exit on the left side.

Figure 16: Case 5 mandible fragments as reconstructed (left) and showing perforation of the left mandibular body (right)

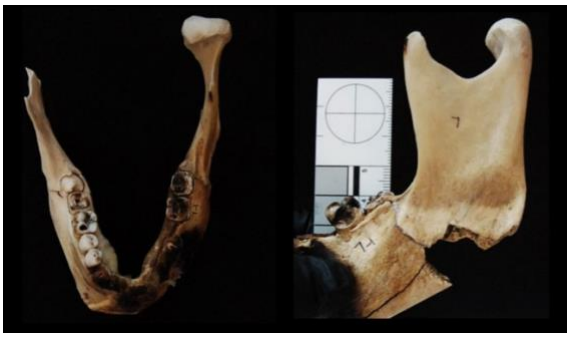

Figure 17: CT imaging of the Case 5 mandible showing the cone crack on the left mandibular body (left and middle) and irregular perforating alteration of the right mandibular body (right)

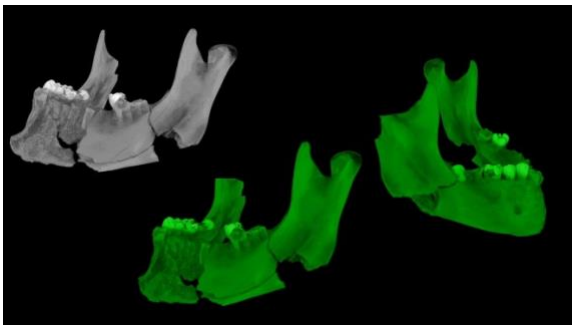

The posterior edge of the exit cone crack exhibits angulation of the EnCF and ExCF (Fig. 18), with some angulation of the EnCF deeper in the cortex. The ExCF is only slightly angulated but situated peripherally to the EnCF, providing a small degree of bevelling. The cortical plates show no signs of compression or delamination which is consistent with the high loading rates associated with projectile trauma.

Figure 18: Cross sectional view of the cone crack in the Case 5 mandible showing angulation of the cone crack margins

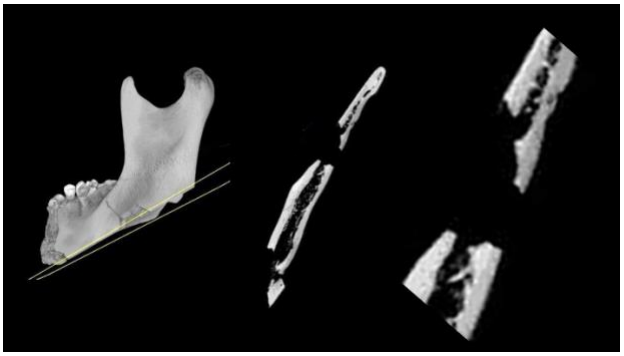

Discussion and Conclusions

These cases demonstrate the cone cracking failure mechanism in human crania impacted at high and low velocities. Moreover, the uses of CT imaging in clarifying the failure mechanism in such cases is highlighted. The differential diagnosis and interpretation of skeletal trauma represent particularly challenging areas of forensic anthropological analysis [25]. Some of this difficulty arises in part from the fact that different actions can produce similar modifications to bone [25]. Skeletonized remains may also be subjected to multiple taphonomic processes that can both damage traumatic features and result in features that mimic them. The production of cone cracks at both low and high velocities also poses important diagnostic challenges [4]. In order to assist practitioners with such difficulties, it is important that traumatic or potentially traumatic features are examined in great detail utilizing new and evolving technologies. Maximum extraction of information of evidentiary value may require analysis with more than one imaging technique [26]. Cone crack geometry has been noted to vary with factors such as projectile velocity and impact angle [27], as well as the material's Poisson's ratio, shear stresses, structure thickness, and method of support [28]. Future work could therefore involve the investigation of these as well as other

extrinsic and intrinsic factors that may influence cone crack geometry [29], for example differences related to biological profile or taphonomy.

As demonstrated in the cases presented here, cross-sectional morphology revealed by micro-CT can yield critical information about crack path, the response of individual laminae to impact, and the behavior of the trabecular layer during the impact event. It can also provide insight into other aspect of the overall fracture pattern such as confirming the presence of concentric heaving fractures that substantiate projectile involvement (as in Case 4), or assist with differential diagnosis when the shape and/or location of a perforation results in an ambiguous etiology (as in the irregularly shaped lambdoidal perforation in Case 3). While it is acknowledged that micro-CT systems may not be commonplace in most forensic laboratory settings, the diagnostic potential provided by their higher resolution indicates that such additional analyses should be considered when skeletal features of ambiguous etiology are being examined. It is hoped that this review provides practitioners with a more thorough understanding of bone beveling and associated fracture patterns, and encourages the analysis of cross-sectional CT imaging in casework.

References

[1] H.E. Berryman, S.A. Symes, Recognizing gunshot and blunt cranial trauma through fracture interpretation, in K.J. Reichs (Ed.), Forensic Osteology: Advances in the Identification of Human Remains, Charles C. Thomas, Springfield, 1998, pp. 333–352.

[2] G.D Quinn, NIST Recommended Practice Guide: Fractography of Ceramics and Glasses, second ed, National Institute of Standards and Technology, Special Publication 960-16e3, 2020.

[3] J.M. Rickman, J. Shackel, A novel hypothesis for the formation of conoidal projectile wounds in sandwich bones, Int. J. Legal Med. 133 (2019) 501–519.

[4] J.M. Rickman, J. Shackel, Crack propagation through sandwich bones due to low-velocity projectile impact, Int. J. Legal Med. 133 (2019) 1443–1459.

[5] A.M. Christensen, J.M. Rickman, H.E. Berryman HE, Forensic fractography of bone: crack origins from impacts, and an improved understanding of the fracture mechanism involved in beveling, Forensic Anthrop. 4 (2021) 67-69.

[6] H. Hertz, Miscellaneous Papers, Translation by D.E. Jones, G.H. Schott, Macmillan and Co. Ltd, London, 1896.

[7] F.C. Frank, B.R. Lawn, On the theory of Hertzian fracture, Proceedings of the Royal Society 299 (1967) 291-306.

[8] B.R Lawn, Indentation of ceramics with spheres: a century after Hertz, J. Am. Ceramics Soc. 81 (1998) 1977-1994.

[9] R. Zaera, V. Sánchez-Gálvez, Analytical modelling of normal and oblique ballistic impact on ceramic/metal lightweight armours. Int. J. Impact Eng. 21 (1998) 133-148.

[10] E.J. Vermeij, P.D. Zoon, S.B.C.G. Chang, I. Keereweer, R. Pieterman, R.R.R. Gerretsen, Analysis of microtraces in invasive traumas using SEM/EDS, Forensic Sci. Int. 214 (2012) 96-104.

[11] B.F. Spatola, Atypical gunshot and blunt force injuries: wounds along the biomechanical continuum, in N.V. Passalacqua, C.W. Rainwater (Eds), Skeletal trauma analysis: case studies in context, John Wiley & Sons, West Sussex, 2015, pp. 7-26.

[12] G. Quatrehomme, M.D Piercecchi-Marti, L. Buchet, V. Alunni, Bone beveling cause by blunt trauma: a case report, Int. J. Legal Med. 130 (2016) 771-775.

[13] J.A. Kieser, J. Tahere, C. Agnew, D.C. Kieser, W. Duncan, M.V. Swain, M.T. Reeves, Morphoscopic analysis of experimentally produced bony wounds from low velocity ballistic impact, Forensic Sci., Med., Path. 7 (2011) 322-332.

[14] M.S. Murphy, C. Gaither, E. Goycochea, J.W. Verano, G. Cock, Violence and weapon-related trauma at Puruchuko-Huaquerones, Peru, Am. J. Phys. Anthrop. 142 (2010) 636-649.

[15] M.S. Murphy, B. Spatola, R. Weathermon, Allies today, enemies tomorrow: a comparative analysis of perimortem injuries along the biomechanical continuum, in D.L. Martin, C.P. Anderson (Eds), Bioarchaeological and Forensic Perspectives on Violence: How Violent Death is Interpreted from Skeletal Remains, Cambridge University Press, Cambridge, 2014, pp. 261-288.

[16] C.E. Bird, J.M. Fleischman, A rare case of an intact bone plug associated with a gunshot exit wound, J. Forensic Sci. 60 (2015) 1074-1077.

[17] A. Kroman, Rethinking bone trauma: a new biomechanical continuum based approach. 62nd Annual Meeting of the American Academy of Forensic Sciences, Chicago, Illinois (2010).

[18] A.M. Christensen, M.A. Smith, D. Cunningham, D. Wescott, D. Glieber. The use of industrial CT in forensic anthropology. Forensic Anthrop. 1 (2) (2018) 124-140.

[19] M.P.S. Machado, M.P. Simoes, T.O. Gamba, I.L. Flores, F.H. Neto, C.H. Duaro, E.D. Junior, E. Cunha, A Wormian bone, mimicking an entry gunshot wound of the skull, in an anthropological specimen, J. Forensic Sci. 61 (3) (2016) 855-857.

[20] S.N. Byers, Introduction to Forensic Anthropology, Boston, MA: Allyn and Bacon (2002).

[21] O.C. Smith, H.E. Berryman, S.A. Symes, J.T. Francisco, V. Hnilica, Atypical gunshot exit defects to the cranial vault. J. Forensic Sci. 38 (2) (1993): 339-343.

[22] O.C. Smith, H.E. Berryman, C.H. Lahren, Cranial fracture patterns and estimate of direction from low velocity gunshot wounds, J. Forensic Sci. 32 (5) (1987): 1416-1421.

[23] G.O. Hart, Fracture pattern interpretation in the skull: differentiating blunt force from ballistics trauma using concentric fractures, J. Forensic Sci. 50 (2005) 1276-81.

[24] H.E. Berryman, A systematic approach to the interpretation of gunshot wound trauma to the cranium, Forensic Sci. Int. 301 (2019) 306-317.

[25] L. Loe, Perimortem trauma, in: S. Blau, D.H. Ubelaker DH (Eds), Handbook of Forensic Anthropology and Archaeology. Walnut Creek, CA: Left Coast Press Inc, (2009): 263–283.

[26] G.N. Rutty, Brough A, Biggs MJP, Robinson C, Lawes SDA, Hainsworth SV. The role of micro-computed tomography in forensic investigations, Forensic Sci. Int. 225: 60-66[27] M.M. Chaudhri. Dynamic fracture of inorganic glasses by hard spherical and conical projectiles. Philosoph. Trans. R (373:20140135) (2015) http://dx.doi.org/10-1098/rsta.2014.0135.

[28] A.C. Fischer-Cripps. Introduction to contact mechanics. Mechanical Engineering Series. Boston: Springer, 2007.

[29] A.M. Christensen, M.I. Isa, M.A. Smith, J.T. Hefner, H.E. Berryman, I.S. Saginor, J.B. Webb. A Guide to Forensic Fractography of Bone (1.0). https://doi.org/10.5281/zenodo.6013748.